Effect of Acoustic Excitation of Gas Flow in a Gas-Centered Swirl Coaxial Injector

Santanu Kumar Sahoo*[1], Shubham Chauhan[1], Hrishikesh Gadgil[1], Sudarshan Kumar[1], K. S. Biju Kumar[2]

[1]Department of Aerospace Engineering, Indian Institute of Technology Bombay, Mumbai 400076, India
[2]Liquid Propulsion Systems Centre, Indian Space Research Organisation, Thiruvananthapuram 695547, India
*Corresponding author email: santanu.s@aero.iitb.ac.in

Abstract
We investigate experimentally the effect of periodic perturbations on the gas flow and assess the possible coupling between the chamber acoustics and the atomization process in a recessed gas-centered swirl coaxial (GCSC) injector by studying the liquid sheet breakup dynamics. Experiments are conducted using water and air, and acoustic perturbations are introduced to the gas flow line using a speaker. High-speed imaging is used for flow diagnostics. The steady spray is observed to transform into a pulsating spray by the acoustic excitation of the gas flow. This pulsating spray resulting from the gas flow perturbations occurs at much lower MFR where the self-pulsation of spray is otherwise not observed without acoustic forcing. The characterization of spray pulsation frequency shows that it matches well with the acoustic frequency. The pulsation effect is more severe with an increase in the MFR. It is further noted that the periodic pulsation of spray exists up to a certain excitation frequency of the gas flow, and beyond this frequency, the dominant pulsation frequency disappears. The atomization process is further quantified in terms of the waviness of the liquid sheet (tortuosity) and the spray turnback angle, which show significant changes in the presence of acoustic excitation.

Keywords
Acoustic excitation, spray pulsation, tortuosity, pulsation frequency

Introduction

Proper atomization is crucial for the efficient working of an engine and hence its investigation is essential for improving the performance. In rocket engines, different types of injectors are used for this purpose [1]. The configurations of injectors vary from impinging jet type injectors to coaxial injectors primarily. However, a particular injector is used based on application and propellant types. Different configurations of coaxial injectors are in use. Specifically, these injectors are used when there are either liquid-gas based or liquid-liquid based propellants. In such systems, one of the propellants flows at a higher velocity to enhance the instability and hence improve the atomization [2]. Usually, the gas velocity is higher than the liquid velocity in gas-liquid based injectors. A very common injection and atomization technique among the coaxial injectors is the swirl coaxial injectors, where, when the gaseous propellant is at the center and the swirling liquid propellant exits from the annular space it is known as a gas-centered swirl coaxial (GCSC) injector. This injector is used for the current study owing to its reliable use in the rocket engines with oxidizer-rich staged combustion cycle [3].
Different studies have aimed to characterize GCSC injectors. Among these, a few notable studies are stated here. Lightfoot and coworkers [4, 5, 6] have studied quite extensively on the GCSC injector to characterize the spray. Kulkarni et al. [7] studied the sheet features like breakup length, spray width, corrugations on the sheet and spray width contraction in a flow through the GCSC injector. They underlined the effect of the gas Reynolds number in its variation and explained the mechanism affecting these sheet behavior. Further, Sivakumar

and Kulkarni[8] identified four regimes of breakup in a non-recessed GCSC injector. They are wave-assisted, perforated, segmented and pulsation regimes with increasing gas momentum. In this non-recessed configuration, the interaction between the liquid and gas phases occurs outside the injector. On the other hand, in a recessed injector, the liquid-gas interaction takes place inside the injector (internal mixing) when the gas flow is sufficiently high [9]. Some studies have simulated conditions closer to the real combustors by investigating effects of flow through GCSC injector in high-pressure environment [10] and using supercritical fluids [11, 12]. They emphasize the importance of the geometrical parameters and give insights into the physics of the flow. Son et al. [13] compared the experimental spray characteristics with numerical results by varying the injection parameters and identified different flow features. Recently the studies on drop-size characteristics have been done by Joseph et al. [14]. Park and coworkers' studies on the acoustic fluctuation of the gas flow [15] and mechanical pulsating of liquid flow [16] reveals the selective response of liquid sheet to few frequencies of excitation. However, it is still unclear how the dynamics of break up get affected by such external forcing.
While proper atomization is the most desirable outcome of an injector, a steady process in achieving this objective is equally important in a liquid rocket engine for a smooth combustion process. Often combustors in rocket engines are known to show acoustic fluctuations. The injector characteristics may be an important contributor to this undesirable phenomenon. The GCSC injector is widely used in liquid propellant rocket engines due to good atomization characteristics and quite a steady flow behavior. However, few studies have also reported the nonuniformities and unsteadiness of flow through this injector. For instance, Lightfoot et al. [17] observed these behaviors for a fully developed spray from a GCSC injector. Also, this is evident from the studies of Sivakumar and Kulkarni [8], where they have identified a pulsation regime of breakup as well, among other regimes. The pulsation regime is seen when the momentum flux ratio (MFR) is sufficiently high. Sahoo and Gadgil [18] characterized this self-pulsation for various injector configurations and flow conditions. They also identified the dominant frequency of pulsation for a certain range of MFRs and some configurations. These studies clearly indicate that there can be some unsteadiness in GCSC injectors. It is worth emphasizing here that the fluctuating chamber acoustics often leads to perturbations in the gas flow which ultimately influence the atomization characteristics and may also affect the combustion stability. This mode of fluctuation of flow in injectors is different from the self-pulsation as it is initiated by external forcing. However, the impact of such a phenomenon may be catastrophic for the combustor. Very little knowledge is available in the literature in this regard considering the fact that a proper understanding is very essential for smooth engine operations. Hence, the objective of the present work is to introduce periodic perturbations to the gas flow and do a preliminary assessment of the possible coupling between the acoustic forcing and the atomization process in a GCSC injector.

Experimental set-up and methodology

Experiments were conducted by using an injector designed in-house. The schematic of this injector is shown in Fig. 1(a). The dimensions are: D_o = 7mm, D_i = 4.5 mm, D_s = 22mm, l_t = 0.5 mm, x, y = 1 mm. A swirler is provided to give a tangential component to the annular liquid flow. The swirling intensity is characterized by the swirl number given by S = $\frac{\pi D_o D_s cos\alpha}{4nxy}$. α is the helix angle of the slot, n is the number of slots, x and y are the slot width and depth. The experiments were conducted at a swirl number of 29.7 and recess ratio (L_R/D_o) of 1 in these experiments. Water and air were used as simulant fluids. Water was pressurized by air to get a steady flow at the exit of the injector. The flow was controlled by a calibrated rotameter. A liquid flow rate of 2.1 LPM was maintained. The coaxial air jet was supplied from a storage tank and desired amount of flow was achieved by passing it through a mass flow controller. Air was allowed to pass through the injector resulting in the momentum flux ratio (MFR) of 2 and 2.2. These MFRs are before the onset of self-pulsation as shown in Fig. 15(b) of [18]. The experimental set up is shown in Fig. 1(b). The flow diagnostics method includes capturing

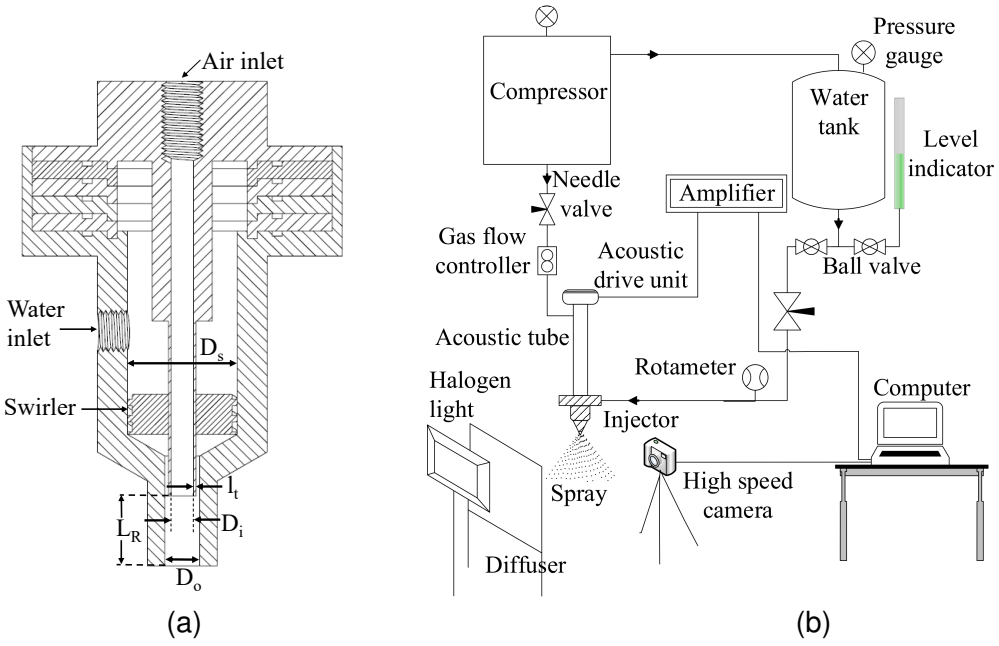

Figure 1. Schematic of experimental facility (a) Cut-section of GCSC injector. (b) Experimental setup for flow visualization.

the shadowgraphic images by a high-speed camera(IDT NX4S2-M-3.0GB-O4) and a Nikon AF Nikkor 50mm f/1.4D lens. The camera was set up at an exposure time of 30 μs and a capturing rate of 8000 frames per second. The image resolution was maintained at 256$\times$256 pixels. The corresponding physical resolution is 4 pixels/mm. The light source was a 1000 W halogen light to a obtain constant intensity of light. For a uniform brightness throughout the captured window, a diffuser screen was placed between the spray and the camera. For individual cases, 5000 images were captured.

The acoustic excitation mechanism consisted of a specially designed acoustic tube, amplifier and an acoustic drive unit (Ahuja AU-60) which is mounted at the top of the injector as shown in Fig. 1(b). Air was made to pass through this tube before entering the injector. Acoustic excitation was created with the desired frequency and sound pressure level. The frequency ranges tested here varied from 600 Hz to 3500 Hz at an interval of 100 Hz. The sound pressure levels (SPL) tested here are 110 dB, 117 dB and 120 dB. It was observed that few small frequency excitations couldn't reach the required amount of SPL from the drive unit. Hence, this study is limited to those frequencies where the above mentioned SPLs could be achieved. The observed changes in the spray pattern are studied by capturing the images. Image processing for the analyses is done using in-house MATLAB codes.

Results and discussion

Characterization of sheet features helps to identify various regimes of sheet breakup in a GCSC injector [8]. A similar approach is therefore taken here to understand the initial impact of acoustic excitation on sheet dynamics. Different morphological changes which a gas-centered swirl coaxial (GCSC) injector undergoes with an increase in the MFR are shown in Fig. 2. Corresponding MFRs are shown below each image. Wave-assisted (MFR = 0), perforated (MFR = 1.2), segmented (MFR = 2.4) and pulsation(MFR = 2.8) regimes are seen in these images. It can be ascertained from these images that the self-pulsation regime starts after MFR = 2.4. Sample images of the sheet shape, when excited by different frequency of acoustic excitation, is shown in Fig. 3. The images shown here are for momentum flux ratio (MFR) = 2.2, which is before the start of self-pulsation regime (c.f. Fig. 2), and SPL = 110 dB. Fig. 3(a) shows the case of an unexcited sheet. Fig. 3(b)-(d) represents the sheet feature at an excitation frequency of 600 Hz, 1000 Hz and 1300 Hz respectively. It can be noticed that while the unexcited sheet does not have significant waves on its surface, the excited sheet can be seen to have

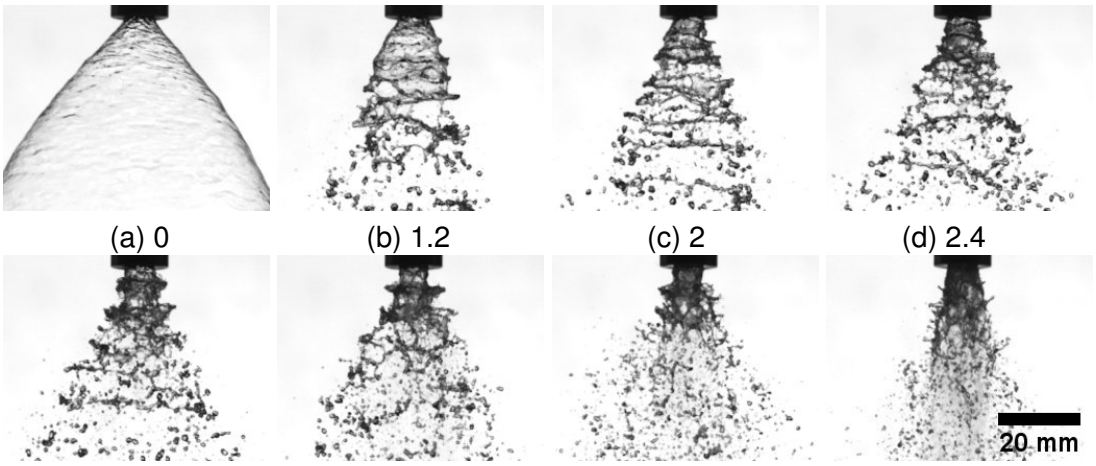

Figure 2. Liquid sheet formed by GCSC injector at different MFR without excitation. MFR values are mentioned below individual images.

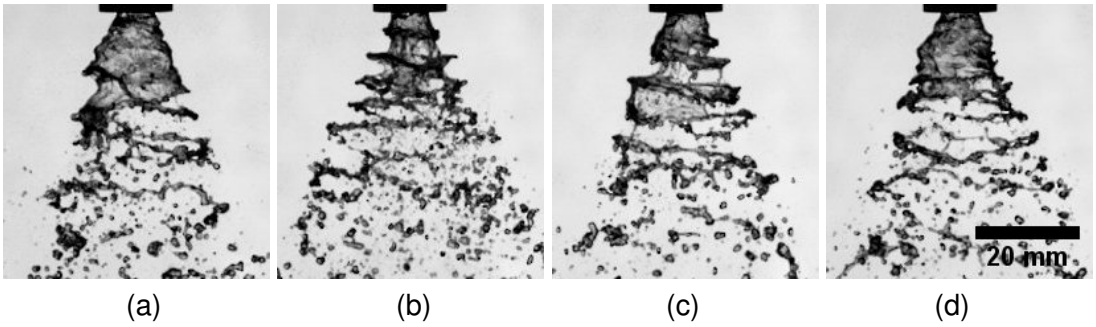

Figure 3. Liquid sheet formed by GCSC injector at different frequency of excitation for MFR = 2.2 and SPL = 110 dB (a) No excitation (b) 600 Hz (c) 1000 Hz (d) 1300 Hz

significant waves/pulses. Interestingly, the wavy structure is not so prominent at a frequency of 1300 Hz and higher. The basic analysis that needs to be done here is the presence of any dominant frequency of occurrence of such pulses. To evaluate this, a binary image is obtained from the original image by considering a threshold value and filling the holes as shown in Fig. 4(a),(b). The sheet width is calculated at 3.5 mm from the orifice. The location is shown by a white horizontal line in Fig. 4(b). This process is repeated for an ensemble of 4000 consecutive images. A time-series data of the width obtained by this procedure is shown in Fig. 4(c). Subsequently, Fast Fourier Transform of this data is carried out to obtain the dominant frequency as shown in Fig. 4(d).

The frequency plots are shown in Fig. 5 for corresponding images in Fig. 3. It can be observed that there is no dominant frequency for the unexcited sheet (Fig. 5(a)). On the introduction of acoustic excitation, a distinct peak in the frequency spectrum appears(Fig. 5(b),(c)). It is important to note here that the dominant frequency is the same as the excitation frequency. Hence, it can be inferred that the wave appearing on the liquid-gas interface in the excited case is due to the acoustic forcing, and is different from self-pulsation frequency which occurs at higher MFR. The response of the liquid sheet to acoustic excitation gradually subsides with the increase in excitation frequency. This can be seen from Fig. 5(d).

Figure 6 shows the frequency response for different MFRs and SPLs at an excitation frequency of 800 Hz. Comparing Fig. 6(a) with (b) and (c) with (d), it is observed that increase in MFR also leads to an increase in the energy content of the dominant frequency. A similar comparison of Fig. 6(a) with (c) and (b) with (d) reveals that it is difficult to comprehend the effects of SPL on the pulsation as the peak amplitude of excitation frequency slightly increases with an increase in SPL for the first comparison and decreases for the other. The reason for this may be the variation of SPL with changing frequency, and hence may be slightly different (less) for the high

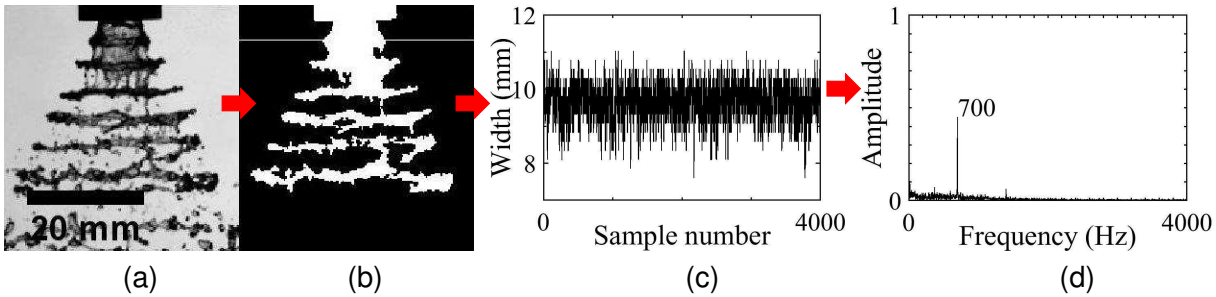

Figure 4. Method for identifying the dominant frequency from the pulses

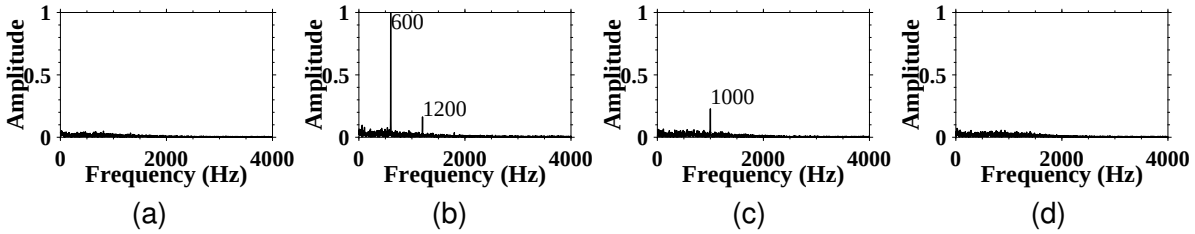

Figure 5. Frequency response of sheet by acoustic excitation of SPL = 110dB and different frequency for MFR = 2.2 (a) No excitation; (b) 600 Hz; (b) 1000 Hz; (b) 1300 Hz

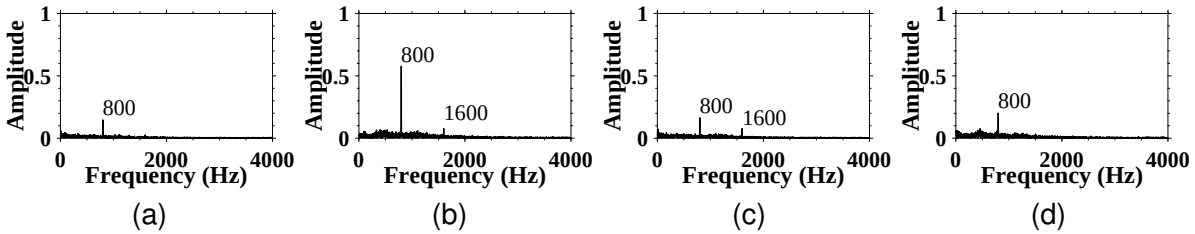

Figure 6. Effect of MFR and SPL on sheet excitation of 800 Hz (a) MFR = 2, SPL = 110 dB; (b) MFR = 2.2, SPL = 110 dB; (c) MFR = 2, SPL = 117 dB; (c) MFR = 2.2, SPL = 117 dB

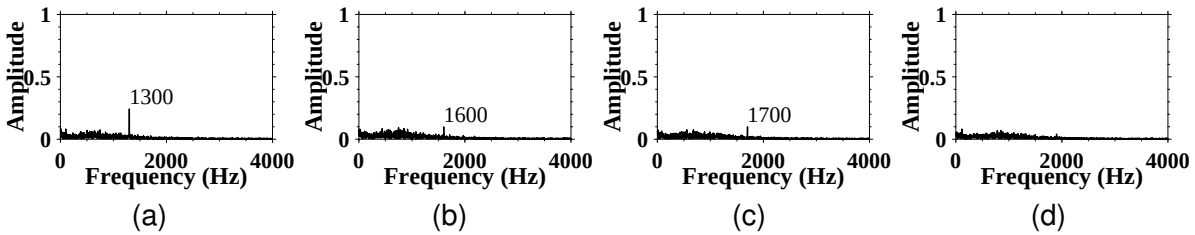

Figure 7. Effect of acoustic excitation of various frequencies at 120 dB on a flow of MFR = 2.2 (a) 1300 Hz; (b) 1600 Hz; (c) 1700 Hz; (d) 1900 Hz;

SPL case. Frequency response of the sheet for various excitation frequencies at MFR = 2.2 and SPL = 120dB is shown in Fig. 7. This shows the dominant frequency at the corresponding excitation frequency. It is observed that the peaks in the frequency spectrum cease to exist when the excitation frequency is above 1800 Hz. The comparison of the range over which dominant peaks exist in case of excitation at 110 dB (Fig. 5) and 120 dB (Fig. 7) suggests that the liquid sheet responds over a wider range of frequency of excitation at a high SPL. It is important to mention here that the acoustic excitation system couldn't reach an SPL of 120 dB for frequencies less than 1300 Hz. However, based on the study of the other two SPLs, it can be ascertained that the sheet is expected to respond to lower excitation frequencies. An interesting observation is that though the excitation of the gas flow is by a monochromatic sine wave generator, in few cases, the presence of another peak with lesser energy at double the frequency value of the primary mode indicates that the pure sinusoidal wave alters to a wave with higher harmonics, which means the perturbed surface does not behave like a pure harmonic one.

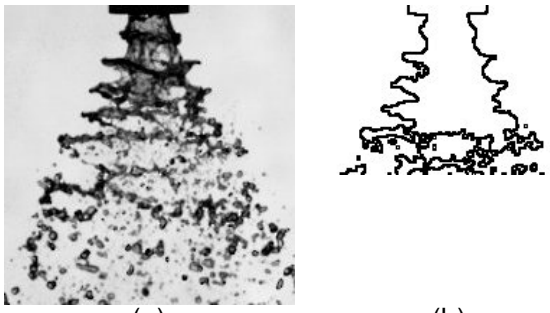

(a) (b)

Figure 8. Detection of boundary of continuous sheet (a) Actual flow (b) Boundary of sheet only

Along with the frequency response of the sheet, there are other changes in the dynamics of the sheet breakup when the gas flow is excited in a GCSC injector. While the frequency studies have their importance in assessing combustion stability, features like breakup and spray spread are equally important for a good performance of the engine. It is well understood that sheet instability is crucial for an easy breakup of bulk liquid. The instability of a liquid sheet can be seen by observing the waves or corrugations. An increase in the waviness of the sheet signifies an increased instability and an increased sheet length for the same sheet height. The consequence of such a sheet behavior can be improved spray features. Quantification of this feature can provide further insights into the effect of acoustic excitation on atomization. Hence, studies are carried out to understand the effect of excitation on the waviness of sheets. It is called as tortuosity [7]. The method of finding tortuosity is by tracing both the edges (Fig. 8) up to the continuous sheet length and finding the average of all images for a case. It can be written as

$$\text{tortuosity} = \frac{\sum_{k=1}^{n-1}\sqrt{(x_{k+1}-x_k)^2+(y_{k+1}-y_k)^2}}{\sqrt{(x_n-x_1)^2+(y_n-y_1)^2}} \tag{1}$$

where x_1, y_1 to x_n, y_n are the coordinates of the edge [8]. While the tortuosity can provide information about the early stage of the breakup when the sheet is intact, what happens beyond the sheet existence region also plays an important role in determining the quality of combustion. After the break up of the liquid sheet, the ligaments and droplets generated travel downstream and undergo combustion in a combustor. It is essential that proper distribution of the spray takes place as droplets and ligaments convect downstream. This requirement of proper spreading of the spray necessitates that in addition to the breakup features, an evaluation of the dispersion characteristics of this broken-off liquid mass is also undertaken. This study can provide important information which can be useful in the design of injectors. Therefore we measured the cone angles for excited and unexcited cases to understand the effect of acoustic excitation. For measuring the cone angle, the average intensity is found by considering all the images for the case as shown in Fig. 9. The tangent of both sides of the sheet ($\alpha_{\text{l}} = tan^{-1}(m_l)$ and $\alpha_{\text{r}} = tan^{-1}(m_r)$) is found at a location from the orifice, and the cone angles are given by

$$\theta_{\text{i}} = \alpha_{\text{l}} + \alpha_{\text{r}} \tag{2}$$

where subscripts *l* and *r* represent the left and right side of the sheet respectively, and subscript *i* denotes the location of measurement of cone angles from the orifice. Though there is significant visible spray spread variation (Fig. 3), however, it didn't get reflected in the cone angle measurements properly. This can also be seen in Fig. 9, where an unexcited and an excited case is shown. It can be noted that the cone angle which is measured near the orifice is quite the same for both cases. So, the turnback angle of the spray is investigated, which is defined by $\theta_{5\text{ mm}} - \theta_{25\text{ mm}}$ to better understand the spray behavior.

The values of tortuosity for different MFRs, SPLs and frequencies are shown in Fig. 10(a). The acoustic force through the gas flow imparts periodic perturbations, which are expected to

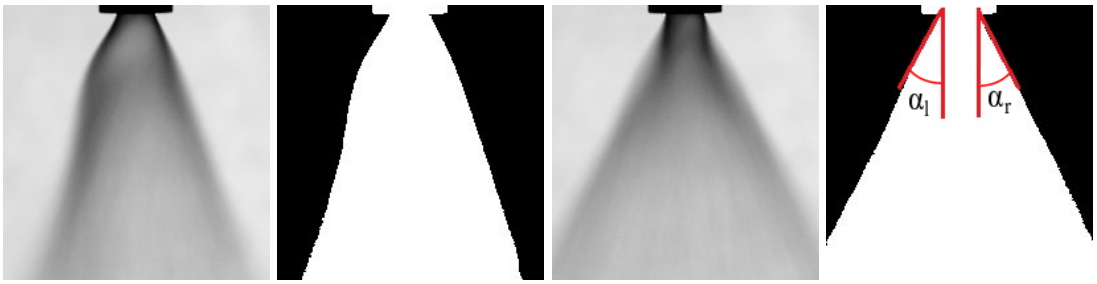

Figure 9. Liquid envelope formed by GCSC injector at different frequency of excitation for MFR = 2.2 and SPL = 110 dB for measuring turn back angle (a) No excitation, average image; (b) No excitation, binary image; (c) 600 Hz, average image; (d) 600 Hz, binary image. α_l and α_r are shown at 5 mm from the orifice.

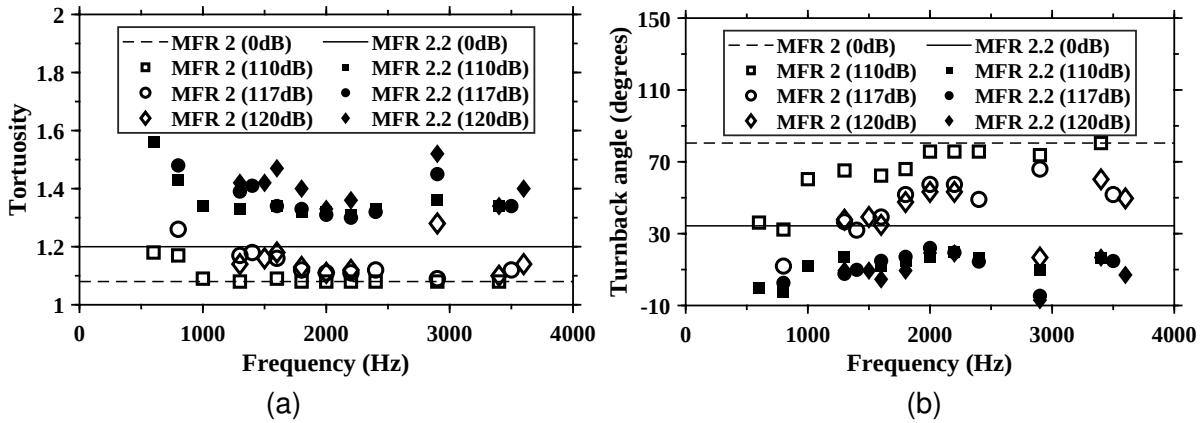

Figure 10. Effect of acoustic excitation on sheet features (a) Tortuosity (b) Turnback angle

enhance instability of the liquid sheet through the generation of more waves. Hence, it can be seen that the tortuosity value is higher for the excited cases than the unexcited ones. The increase in MFR translates into the increase in shear between the two fluids which increases the corrugations in the liquid sheet and results in an increase of tortuosity value. Note that the tortuosity values though remain higher in excited cases than the values at unexcited ones, it decreases with an increase in frequency at lower frequency values. These values almost reach the unexcited sheet values for low MFR. Basically, the difference in tortuosity between excited and unexcited sheets is more in the case of flow with higher MFR. The reason for such behavior could be the increased amplitude of gas flow perturbations imparted by the acoustic forcing at higher MFR. It is observed that, usually, the higher tortuosity values correspond to the cases with the existence of dominant frequency. The better response of sheet to lower frequencies may be the reason for the decrease in the tortuosity values with an increase in frequency.

The variation of turnback angle for all the investigated conditions is shown in Fig. 10(b). The turnback angles of excited cases are seen to be less than the unexcited case. Also, these values for higher MFR are less than the values for lower ones. A high turnback angle implies the sheet subtends a higher cone angle near the nozzle but contracts further downstream of the flow (Fig. 9(a) and (b)), while the lower turnback angle indicates that the spray follows a straight trajectory from the orifice (Fig. 9(c) and (d)). This feature can also be verified from the actual spray image in Fig. 3. The spray behavior, when the liquid sheet gets significantly affected by acoustic excitation, is quite similar to the spray behavior with higher MFR in an unexcited GCSC injector. The corresponding regime of sheet breakup of the unexcited injector is the pulsation regime. Hence, the phenomenon of lower turnback angle for acoustically excited injector can be understood by considering the fact that the acoustic pulse periodically increases the gas mass flow rate due to periodic pressure fluctuations imparted by the compressions and rarefactions of an acoustic wave. As a result, the liquid mass ejects when subjected to interaction with an effectively high gas flow rate periodically.

Conclusions

The effect of periodic perturbation of gas flow in a recessed gas-centered swirl coaxial (GCSC) injector is studied experimentally using high-speed imaging in this paper. The studies were done with a single value of swirl at a fixed liquid flow rate and two different gas flow rates. Acoustic excitation at three different sound pressure levels (110 dB, 117 dB and 120 dB) and frequency up to 3500 Hz were introduced through the gas channel of the GCSC injector. Qualitative and quantitative studies reveal that the liquid sheet dynamics get affected by acoustic excitations. It is observed that the sheet breakup regime becomes pulsating at a lower momentum flux ratio (MFR) compared to the unexcited cases with self-pulsation. The dominant frequency of pulsation exists only for some range of frequencies of excitation, which matches with the excitation frequency. This indicates that periodic excitation of the interfacial waves occurs only over a range of excitation frequencies. However, the sheet waviness (tortuosity) and the turnback angle are observed to increase and decrease respectively in presence of acoustic excitation of the gas flow. This effect is more prominent in the range of excitation frequencies when the dominant frequency is present. This signifies the role of acoustic excitation in the sheet breakup dynamics for all the cases studied here. The effect of excitation is observed to be more severe with an increase in MFR.

References

[1] Gill, G. S. and Nurick, W. H., 1976, “Liquid rocket engine injectors”. NASA SP-8089.

[2] Lasheras, J. C., Hopfinger, E. J, 2000, *Annual review of fluid mechanics*, 32 (1), pp. 275-308.

[3] Long, M. and Anderson, W., Jul. 11.-14. 2004, 40th AIAA/ASME/SAE/ASEE Joint Propulsion Conference and Exhibit.

[4] Schumaker, S., Danczyk, S. and Lightfoot, M., May. 23.- 26. 2006, Institute for Liquid Atomization and Spray Systems Americas

[5] Schumaker, S., Danczyk, S. and Lightfoot, M., Jan. 4.-7. 2010, 48th AIAA Aerospace Sciences Meeting Including the New Horizons Forum and Aerospace Exposition.

[6] Schumaker, S., Danczyk, S. and Lightfoot, M., Jul. 31.-Aug. 3. 2011, 47th AIAA/ASME/SAE/ASEE Joint Propulsion Conference & Exhibit.

[7] Kulkarni, V., Sivakumar, D., Oommen, C., Tharakan, T., 2010, *Journal of Fluids Engineering*, 132 (1), pp. 011303.

[8] Sivakumar, D., Kulkarni, V., 2011, *Experiments in Fluids*, 51 (3), pp. 587–596.

[9] Jeon, J., Hong, M., Han, Y.-M., Lee, S. Y., 2011, *Journal of Fluids Engineering*, 133 (12), pp. 121303.

[10] Kim, J. G., Han, Y. M., Choi, H. S., Yoon, Y., 2013, *Aerospace Science and Technology*, 27 (1), pp. 171-178.

[11] Zhang, L., Wang, X., Li, Y., Yeh, S.-T., Yang, V., 2018, *Physics of Fluids*, 30 (7), pp. 075106.

[12] Wang, X. and Wang, Y. and Yang, V., 2019, *Physics of Fluids*, 31 (6), pp. 065109.

[13] Son, J., Sohn, C. H., Park, G., Yoon, Y., 2017, *Journal of Aerospace Engineering*, 30 (5), pp. 04017035.

[14] Joseph, A., Sakthikumar, R., Sivakumar, D., 2020, *Journal of Fluids Engineering*, 142 (4), pp. 041206.

[15] Park, G., Lee, J., Oh, S., Yoon, Y., Sohn, C. H., 2016, *AIAA Journal*, 55 (3), pp. 894–901.

[16] Park, G., Oh, S., Yoon, Y., Choi, J.-Y., 2019, *Journal of Propulsion and Power*, 35 (3), pp. 624-631.

[17] Lightfoot, M. D. A. and Danczyk, S. A., Jul. 26.- 30. 2009, International Conference on Liquid Atomization and Spray Systems.

[18] Sahoo, S. K., Gadgil, H., 2021, *Journal of Propulsion and Power*, 37 (3), pp. 450-462.

[19] Matas, J.-P., Hong, M., Cartellier, A., 2014, *Physics of Fluids*, 26 (4), pp. 042108.